Electronic Supplementary Material (ESI) for Physical Chemistry Chemical Physics.

Investigation of nonlinear optical properties in α-$A_2BB'O_6$ (A = Li, Na, K; B= Ti, Zr, Hf; B′ = Se, Te) by first-principles calculations

Gaojing Fang,[ab] Xiaojun Teng,[c] Luo Yan,[ad] Yu Wu,[a] Kui Xue,[ad] Xiaofeng Zhang,[d] Yi-min Ding,*[a] Liujiang Zhou,*[ad] and Qiye Wen*[ab]

[a] Yangtze Delta Region Institute (Huzhou), University of Electronic Science and Technology of China, Huzhou 313001, China

[b] School of Electronic Science and Engineering, University of Electronic Science and Technology of China, Chengdu 610054, China

c Chengdu Answer Information Technology Co., LTD., Chengdu 610041, China

[d] School of Physics, University of Electronic Science and Technology of China, Chengdu 610054, China

1 Table of content

2 The results of AIMD, phonon spectra, band and DOS of stable ABB′O

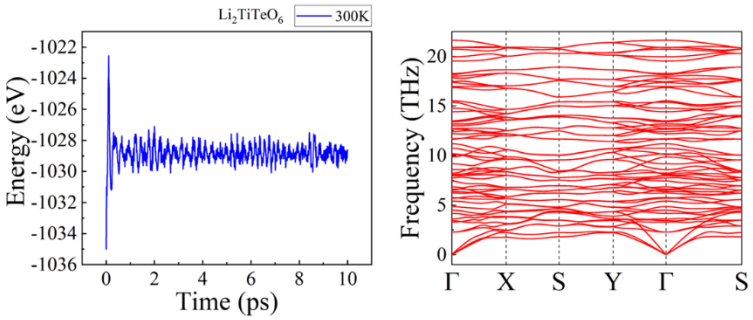

Figure S1. Energy variations under the AIMD simulations and phonon spectra at 300 K of Li_2TiTeO_6 (Band and DOS are presented in main text).

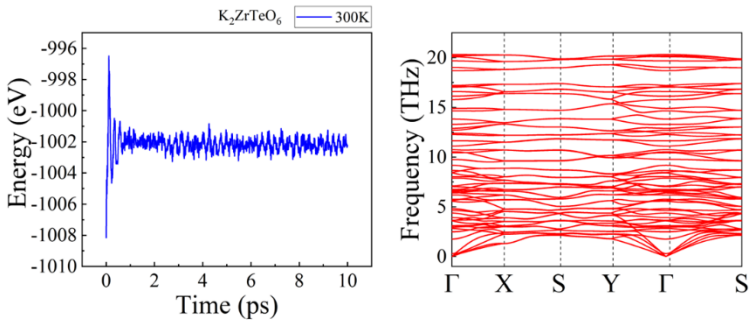

Figure S2. Energy variations under the AIMD simulations and phonon spectra at 300 K of K_2ZrTeO_6 (Band and DOS are presented in main text).

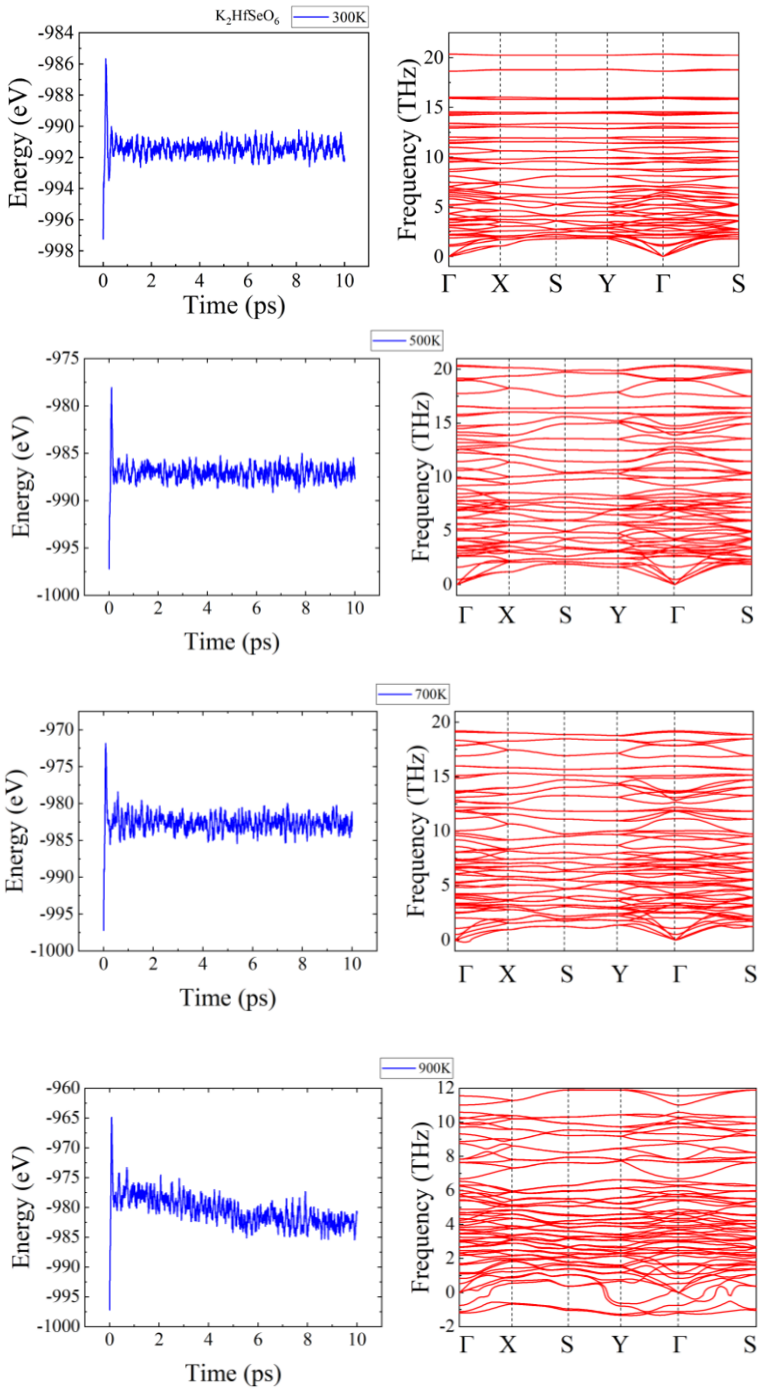

Figure S3. Energy variations under the AIMD simulations and phonon spectra at 300, 500, 700 and 900 K of K_2HfSeO_6 (Band and DOS are presented in main text).

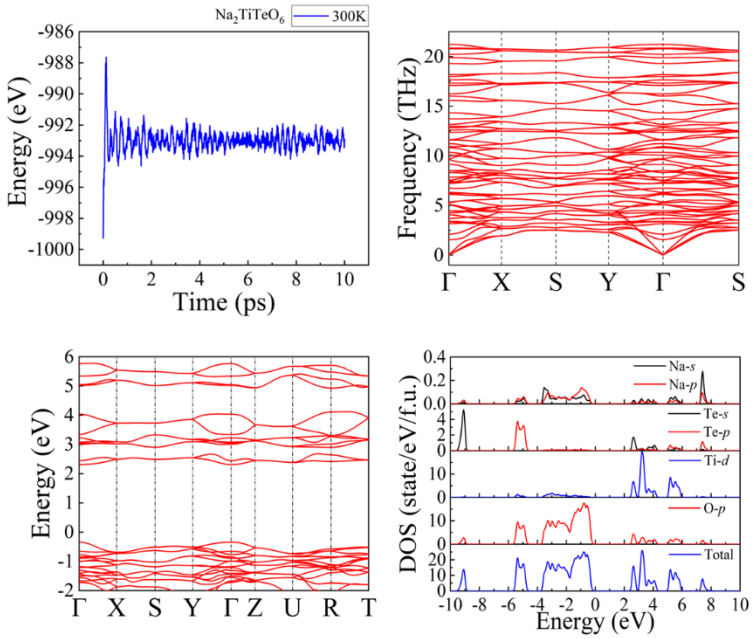

Figure S4. Energy variations under the AIMD simulations and phonon spectra at 300 K of states of Na_2TiTeO_6.

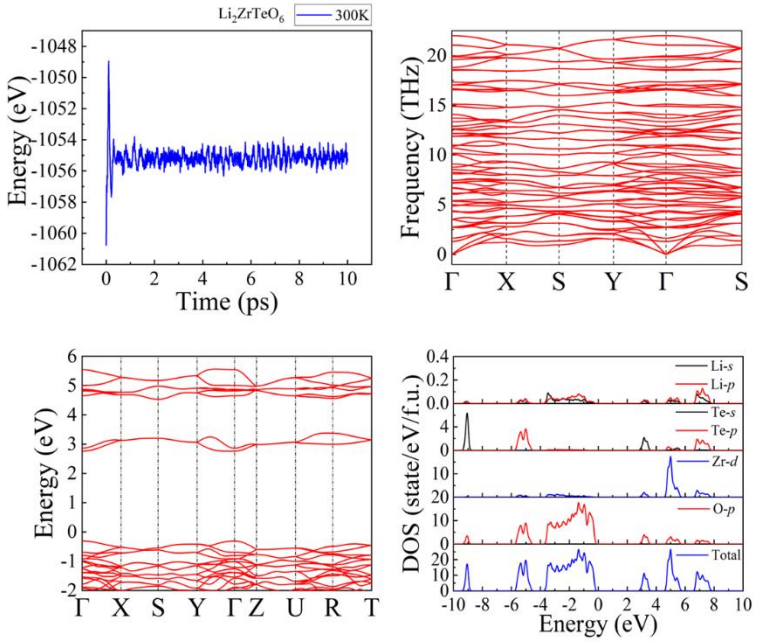

Figure S5. Energy variations under the AIMD simulations, phonon spectra at 300 K, energy band and density of states of Li_2ZrTeO_6.

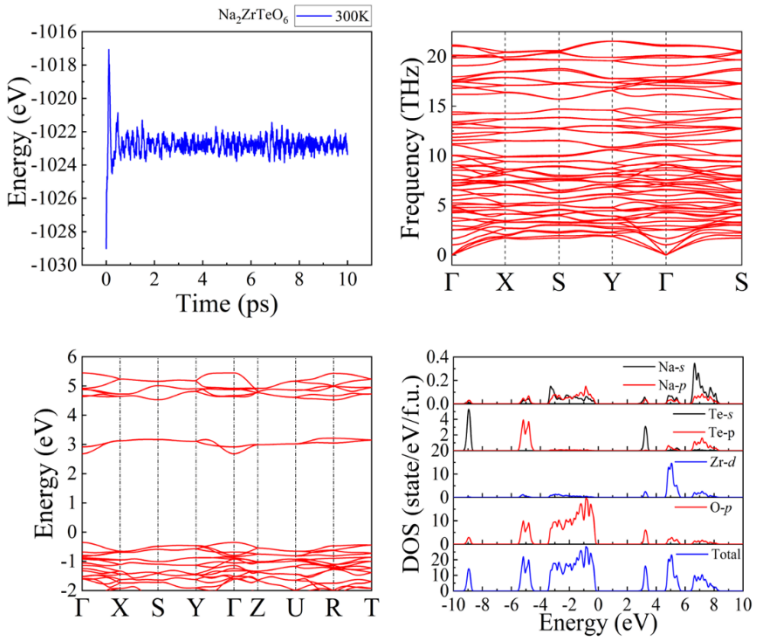

Figure S6. Energy variations under the AIMD simulations, phonon spectra at 300 K, energy band and density of states of Na_2ZrTeO_6.

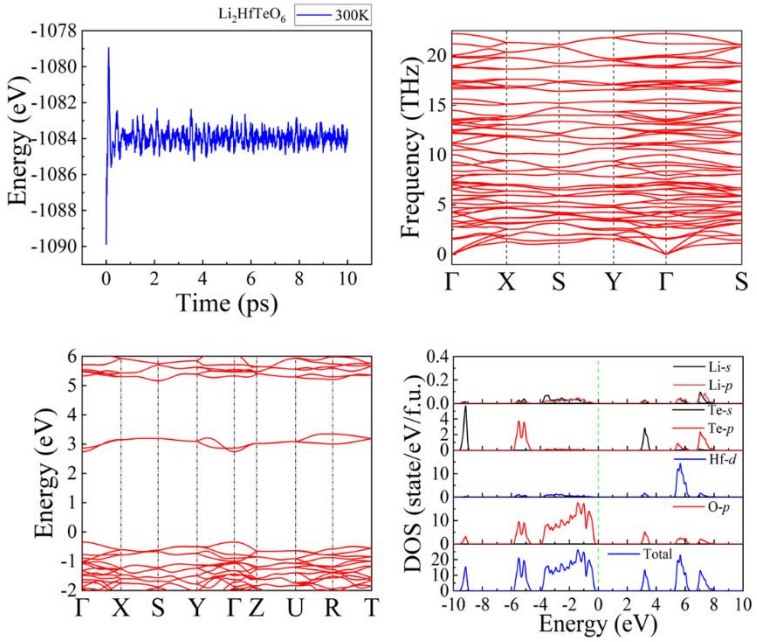

Figure S7. Energy variations under the AIMD simulations, phonon spectra at 300 K, energy band and density of states of Li_2HfTeO_6.

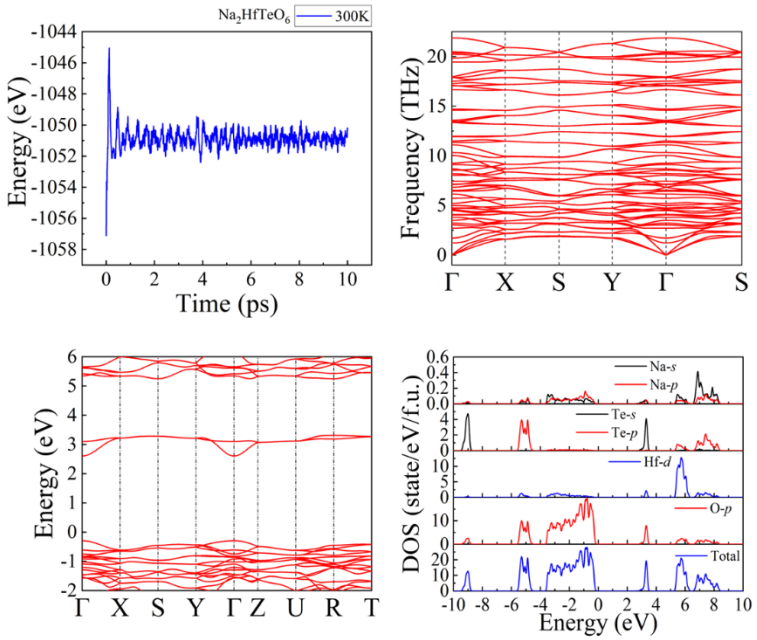

Figure S8. Energy variations under the AIMD simulations, phonon spectra at 300 K, energy band and density of states of Na_2HfTeO_6.

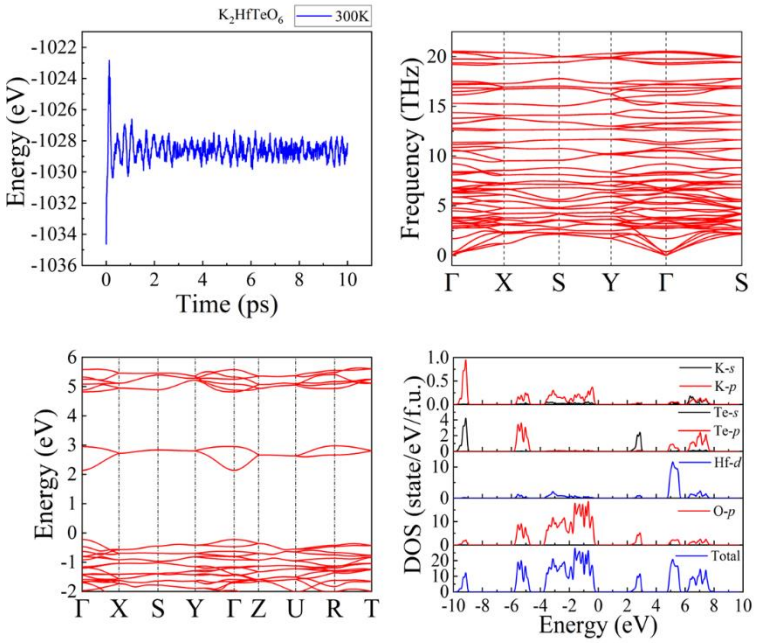

Figure S9. Energy variations under the AIMD simulations, phonon spectra at 300 K, energy band and density of states of K_2HfTeO_6.

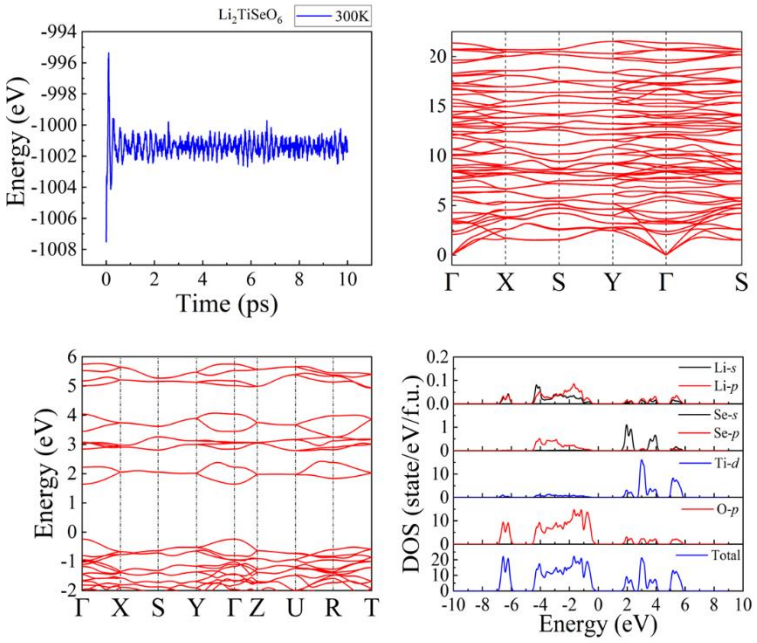

Figure S10. Energy variations under the AIMD simulations, phonon spectra at 300 K, energy band and density of states of Li_2TiSeO_6.

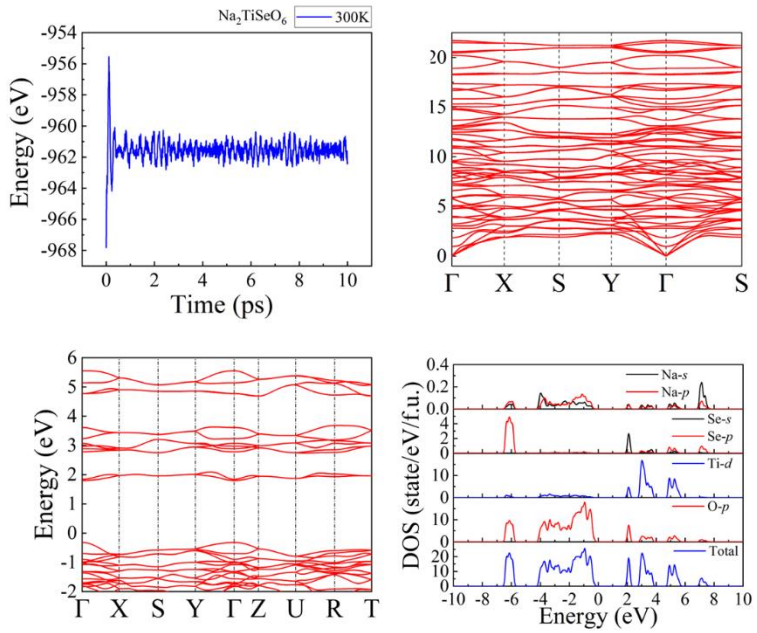

Figure S11. Energy variations under the AIMD simulations, phonon spectra at 300 K, energy band and density of states of Na_2TiSeO_6.

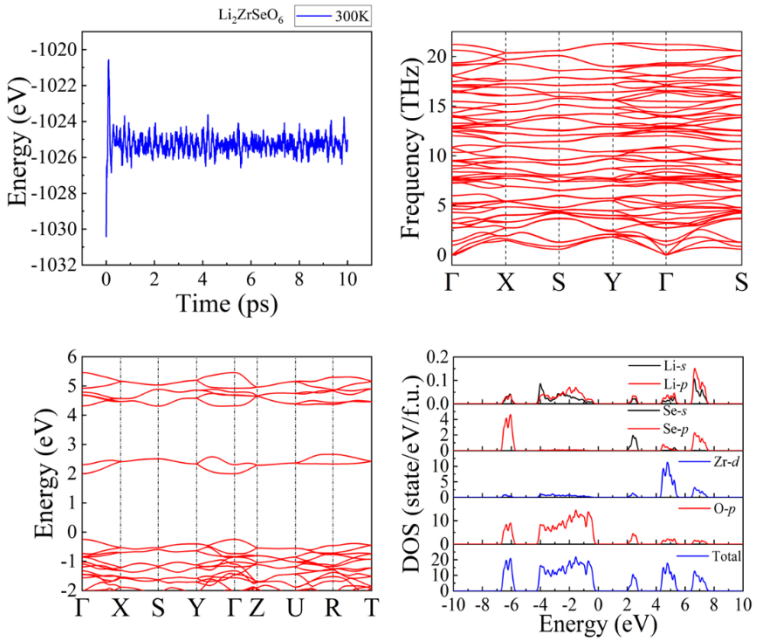

Figure S12. Energy variations under the AIMD simulations, phonon spectra at 300 K, energy band and density of states of Li_2ZrSeO_6.

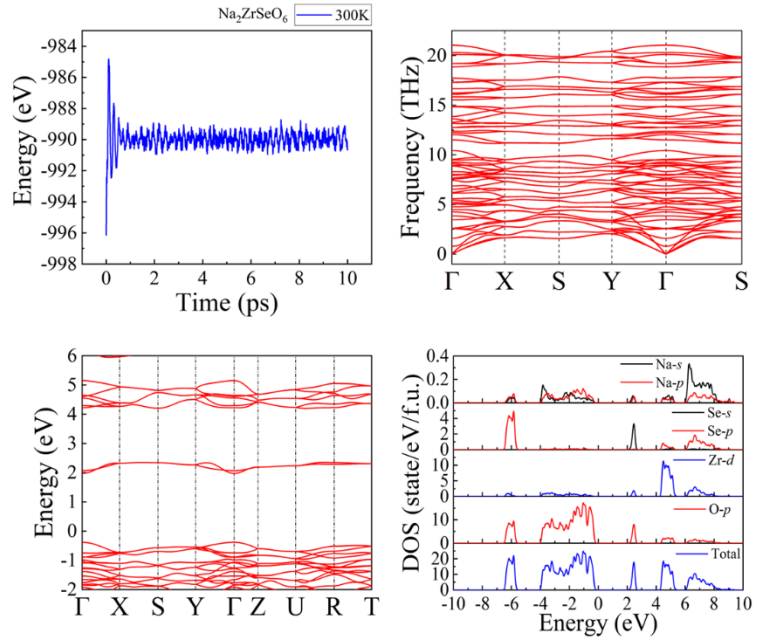

Figure S13. Energy variations under the AIMD simulations, phonon spectra at 300 K, energy band and density of states of Na_2ZrSeO_6.

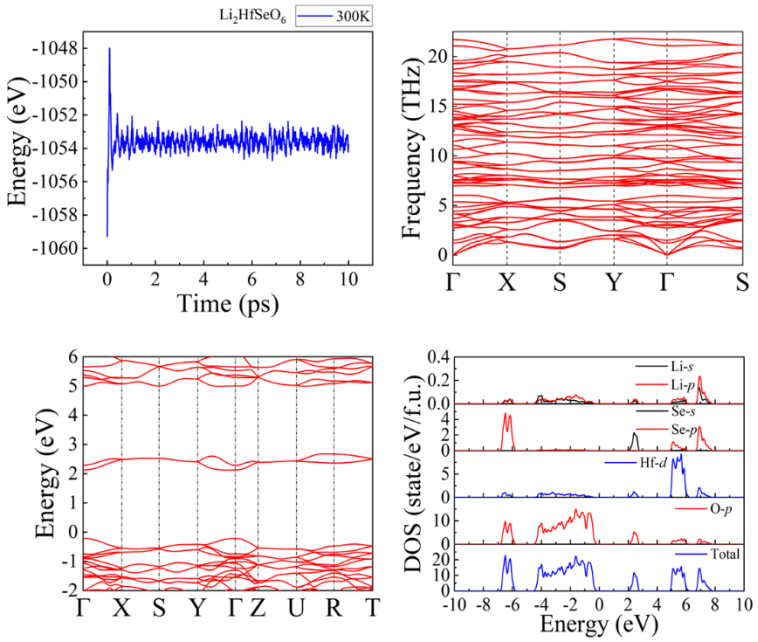

Figure S14. Energy variations under the AIMD simulations, phonon spectra at 300 K, energy band and density of states of Li_2HfSeO_6.

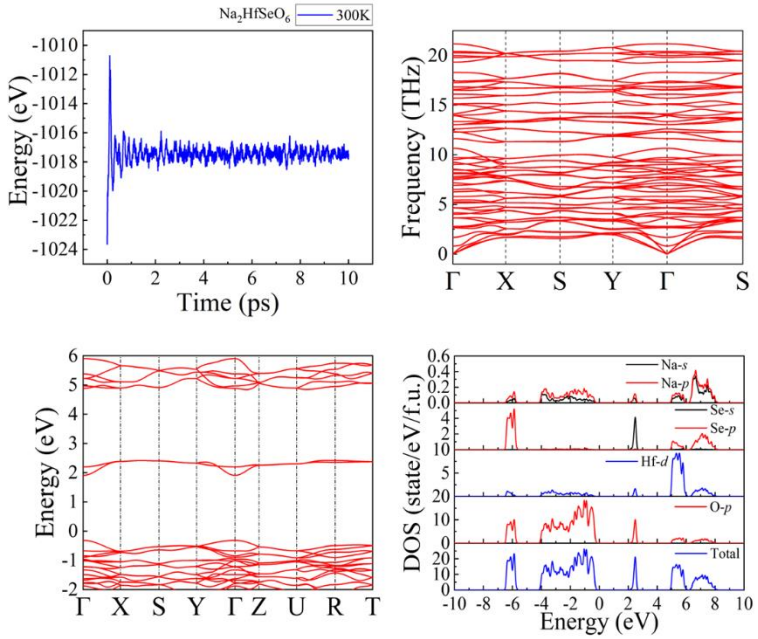

Figure S15. Energy variations under the AIMD simulations, phonon spectra at 300 K, energy band and density of states of Na_2HfSeO_6.

3 The results of AIMD and phonon spectra of unstable ABB′O

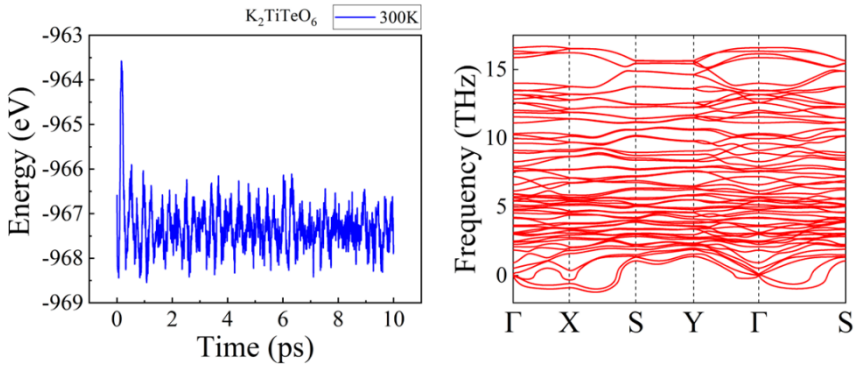

Figure S16. Energy variations under the AIMD simulations and phonon spectra at 300 K of K_2TiTeO_6.

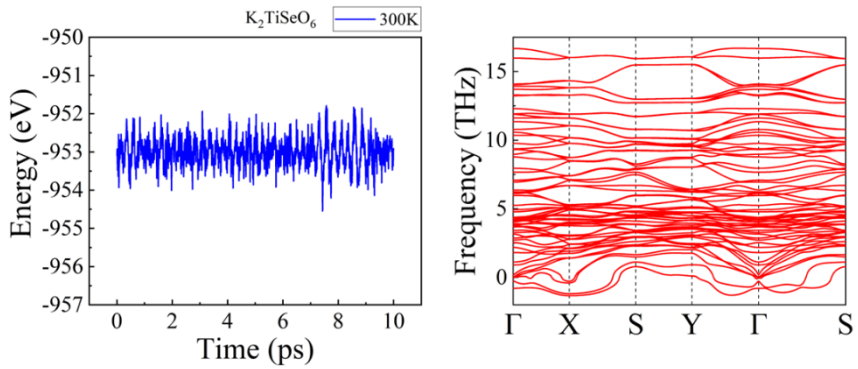

Figure S17. Energy variations under the AIMD simulations, phonon spectra at 300 K, energy band and density of states of K_2TiSeO_6.

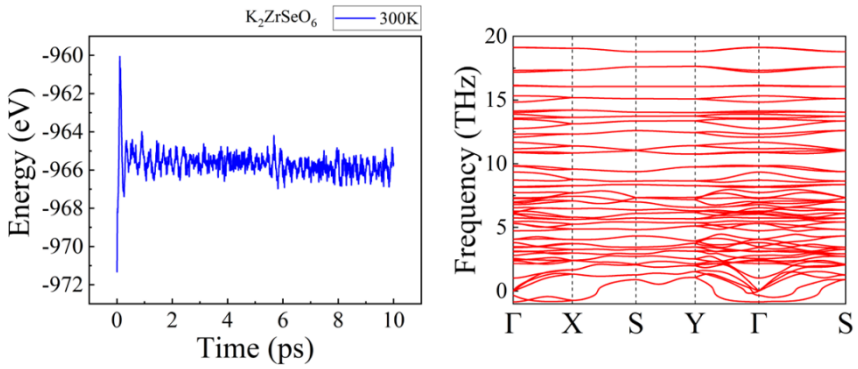

Figure S18. Energy variations under the AIMD simulations, phonon spectra at 300 K, energy band and density of states of K_2ZrSeO_6.

4 Calculated bandgap by different functionals and experimental value for LTTO

Table S1. Calculated bandgap (in unit of eV) by different functionals and experimental value for LTTO

	PBE	PW91	RPBE	PBEsol	AM05	SCAN	MBJ	HSE06	Exp.
LTTO	2.38	2.38	2.43	2.34	2.35	2.81	3.29	3.69	3.67

5 Elastic stiffness constants

Table S2. Elastic stiffness constants C_{ij} of $A_2BB'O_6$

formula	Tensor C_{ij} (GPa)								
	C_{11}	C_{12}	C_{13}	C_{22}	C_{23}	C_{33}	C_{44}	C_{55}	C_{66}
Li_2TiTeO_6	258.82	90.61	116.07	358.51	100.26	261.07	113.53	143.45	122.52
Na_2TiTeO_6	248.27	75.79	98.80	302.78	89.07	219.04	99.13	118.67	96.80
Li_2ZrTeO_6	237.25	92.37	117.53	331.71	103.45	240.35	108.09	136.59	112.99
Na_2ZrTeO_6	228.04	76.42	103.03	291.54	88.16	212.81	94.83	118.25	91.57
K_2ZrTeO_6	247.18	78.97	97.67	263.93	89.18	190.32	93.31	107.69	85.78
Li_2HfTeO_6	244.43	92.85	121.22	350.11	102.27	259.32	114.61	144.70	120.71
Na_2HfTeO_6	242.37	83.21	110.39	314.20	91.42	230.29	103.45	128.93	103.24
K_2HfTeO_6	255.07	80.21	98.65	272.74	89.87	197.08	97.39	110.62	90.73
Li_2TiSeO_6	284.61	80.33	108.60	365.67	100.13	274.59	118.73	141.82	121.57
Na_2TiSeO_6	271.59	68.79	88.26	305.73	90.38	226.73	106.27	113.49	98.68
Li_2ZrSeO_6	265.01	81.35	109.14	337.92	102.12	248.75	111.47	132.54	109.65
Na_2ZrSeO_6	257.55	72.82	96.56	300.13	91.60	220.36	102.43	116.48	94.10
Li_2HfSeO_6	273.71	82.88	113.35	358.63	102.45	267.26	118.44	141.58	118.18
Na_2HfSeO_6	266.19	74.09	98.52	313.90	91.43	231.10	107.91	121.27	101.01
K_2HfSeO_6	273.09	73.94	83.48	269.73	86.96	191.51	100.06	98.01	90.79

6 Total dipole moment of unit cell

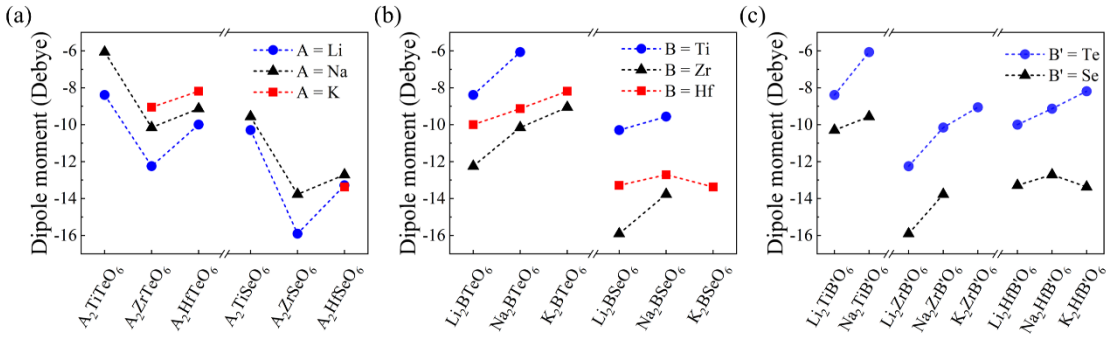

Figure S19. Total dipole moment of unit cell with different atoms at (a) A-site, (b) B-site and (c) B'-site of ABB'O.

7 THz adsorption spectrum of ABB′O

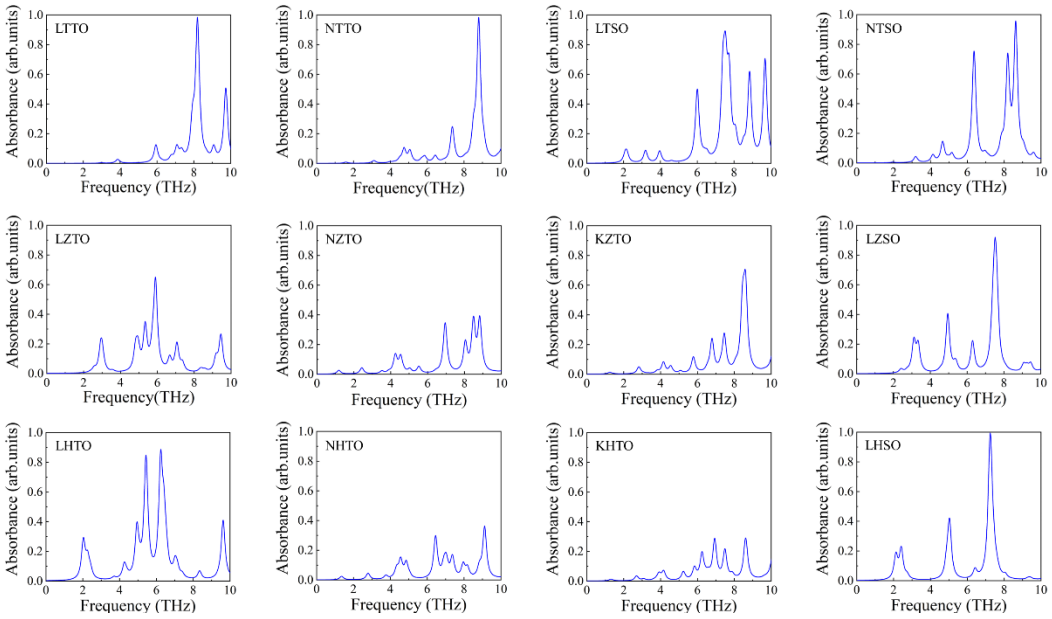

Figure S20. Calculated THz absorption spectra of ABB′O (others are presented in main text).